ISSN 1846-6168 (Print), ISSN 1848-5588 (Online)
https://doi.org/10.31803/tg-20230710223321

Original scientific paper
Received: 2023-07-10, Accepted: 2023-08-04

Analytical Description of the Electric Field inside a High Voltage Glass Insulator

Tomislav Barić, Hrvoje Glavaš, Željko Hederić, Mirko Karakašić*

Abstract: Research presented in this paper analyzes the accuracy and applicability of analytical expressions to describe the electric field of a high-voltage glass insulator. The metal cap and the metal pin of the glass insulator are represented by coaxial cylindrical electrodes. The insulating materials between them are modeled as coaxial hollow cylinders. Analytical expressions for the electric field in these insulating materials are derived. Using these expressions, the spatial distribution of the electric field in the insulating materials was determined. Suitable software, based on the finite element method (FEM), was used to determine the spatial distribution of the electric field in dielectrics in the same space. Both analyses were performed under quasi-static conditions, and the results of the analytical expressions were compared with the FEM results. Discrepancies between the results of the two mentioned analyses were observed. The reasons for the observed discrepancies and the applicability of the presented analytical expressions are commented on.

Keywords: analytical description; electric field; finite element method (FEM); glass insulator; high voltage; numerical calculation

1 INTRODUCTION

The significant development of the electric power grid began in the second half of the 19th century. Since then, the power grid has become more complex and the electric power which is carried from different sources to consumers is getting increasingly higher. To reduce transmission losses, voltage levels have become higher. Reliability and availability are also getting higher. All of the above has become possible with the simultaneous development of all components in the transmission and distribution of electricity. One of the important components in the transmission and distribution of electricity are insulators [1-3].

In this article, when researches talk about insulators, they refer to high-voltage (HV) insulators with the application in the transmission and distribution of electricity. As the mentioned development of the electric power grid took place all the time from applied electricity beginnings, also developments of HV isolators have been continuously improved.

Knowledge of the exact electric field (E-field) distribution is crucial in the process of designing and analysing HV components such as HV insulators. The calculation of E-fields requires the solution of the field formulation according to Maxwell's equations with meeting the boundary requirements [4]. This can be done by applying analytical or numerical methods [5-7]. Due to the geometric complexity of HV components, analytical expressions are rarely applicable [4]. To demonstrate, a short review of the selected examples will be provided. Analytical expressions in HV technology can be used to determine the electric field in the vicinity of HV overhead transmission lines [8, 9]. Also, analytical expressions can be used to determine the induced current densities and voltages in a two-layer soil by an HV transmission line [10]. Since the energy stored in an E-field must be equal to the energy stored in the equivalent capacitance, when the expression for the E-field of a particular geometry is known, the capacitance of this geometry is also known. This enables the application of analytical expressions for E-fields to determine the capacitance of overhead transmission lines [11]. The aforesaid also applies to HV cables [12]. With analytical expressions, it is possible to describe the E-field inside of HV direct current cable insulations, considering a varying conductivity in the vicinity of an interface, e.g. in cable joints, which usually consists of two different dielectrics [13]. Analytical expressions in HV technology can also be combined with the results obtained by numerical methods. This has proven to be particularly suitable for analysing and interpreting the results obtained by numerical methods. For example, by combining analytical expressions and simulation results obtained by the Finite Element Method (FEM), it is possible to analyse and interpret the intensification of the E-field due to the presence of water droplets on the surface of HV insulators [14].

A special advantage of numerical methods, in relation to the analytical ones, is that they enable the analysis of arbitrarily complex geometries and geometric configurations, while certain approximations of geometric shapes are always present in analytical methods. Due to the stated advantages of numerical methods, the use of analytical methods in describing the E-field in insulators has decreased, and has given way to numerical methods in electromagnetism. Today, the use of numerical methods in electromagnetism exclusively dominates the analysis of electromagnetic fields in insulators.

Nevertheless, it is still beneficial to have suitable analytical expressions, although approximate, to describe the E-fields in insulators. Analytical expressions simplify theoretical considerations, indicate functional relations between physical quantities and enable rapid qualitative considerations. At the same time, if they give reasonably (acceptable) accurate results, the results obtained by them can serve as an indicator of the validity of numerical calculation. That is, to check whether there is any error in modelling using numerical methods. This was a strong motivation to investigate whether it is possible, and if yes, how accurately the E-field in the space between the metal cap and the metal pin can be described.

In order to derive analytical expressions that can describe the electric field in the specified zone, an approximation of

the geometry of the specified zone was performed. The metal cap and metal pin are represented by coaxial cylindrical electrodes. The insulating materials between the metal cap and the metal pin (cement and glass) are modelled as hollow coaxial cylinders. Using derived expressions on a concrete example of a disk insulator, the spatial distribution of the E-field in dielectrics was determined. In order to determine the accuracy of the obtained results, the same calculation was performed by the FEM. For this purpose, commercial software Ansys based on the FEM was used. Deviations of the results obtained by analytical expressions in relation to the accurate results obtained by applying the FEM were observed. The underlying reasons for the observed deviations and the applicability limits of the presented analytical expressions are commented on.

2 HIGH VOLTAGE GLASS INSULATORS

Significant progress on several levels has been made since HV insulators were first used. The technological process for producing insulating materials without microdefects and microinhomogeneities has been improved. New insulating materials, such as composite polymers, have been discovered [15, 16]. The insulator geometry has been improved and the surface has been treated with materials (coatings) that reduce their adhesion to the insulator surface [17-19]. This is especially important for porcelain insulators, where moisture and dirt deposits on the surface of porcelain insulators affect the E-field distribution, which can lead to partial discharges. The influence of non-uniform thermal properties of the materials making up the insulators, i.e. non-uniform expansions due to temperature changes causing material stresses and micro-fractures, are minimized by proper design.

Despite advances in the synthesis of polymeric composite insulators with suitable mechanical, thermal and electrical properties for the fabrication of HV insulators, traditionally used materials such as porcelain and glass still dominate in applications. One such glass insulator is described in this article. Common types of HV insulators used in transmission and distribution are pin insulators, shackle insulators, suspension insulators (disk or cord), strain or tension insulators. As for the insulating materials used, insulators for power transmission and distribution HV are made of glass, ceramic materials, such as porcelain, or polymers, also called polymer composites. Sometimes, the insulator name also includes the name of the insulator geometric shape, e.g. disk insulators.

In this article, the focus is on disk-shaped (bell-shaped) insulators. HV cap-and-pin (disk) insulators [2], regardless of which material is chosen as the primary insulator (glass or porcelain), have a similar shape. A typical HV disk insulator (porcelain or glass as the primary insulator material) has the shape of a bell (disk) (Fig. 1 [20, 21]). When the line voltage requires more insulation than a single disk insulator can provide, disk insulators are connected in series.

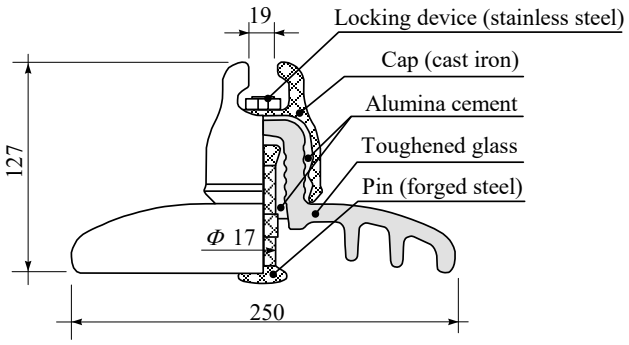

Figure 1 Structure of the analyzed glass disk insulator

3 THEORETICAL BACKGROUND (BOUNDARY CONDITIONS)

Solving electromagnetic problems requires knowledge of the boundary conditions at the boundary between two media with different electromagnetic properties [22-24]. In this section, a brief overview of the boundary conditions at the boundaries of the two media found in the case study analyzed in this article is given. The boundary conditions for an E-field on an interface separating two homogeneous isotropic materials can be written in a concise form [22, 23]:

$$\vec{n} \times (\vec{E}_1 - \vec{E}_2) = 0\,, \tag{1}$$

where $\vec{n}$ is the normal vector to the boundary surface, $\vec{E}_1$ is electric field in medium no 1 next to the boundary surface and $\vec{E}_2$ is electric field in medium no 2 next to the boundary surface. Basically, the previous equation shows that the tangential component of the electric field remains unchanged at the boundary of the two media. That is, the tangential component of the electric field is continuous across the interface (Fig. 2) [23]:

$$\vec{E}_{1,t} = \vec{E}_{2,t}\,. \tag{2}$$

Boundary conditions for electric displacement field $\vec{D}$ on a boundary surface separating two homogeneous isotropic materials can be written in a concise form [23]:

$$\vec{n} \cdot (\vec{D}_1 - \vec{D}_2) = 0\,, \tag{3}$$

where $\vec{n}$ is the normal vector to the boundary surface, $\vec{D}_1$ is electric displacement field in the medium denoted by 1 next to the boundary surface, $\vec{D}_2$ is electric displacement field in the medium denoted by 2 next to the boundary surface. Basically, the previous equation shows that the normal component of the electric displacement field remains unchanged at the boundary of the two media (Fig. 2). That is, the normal component of the electric displacement field $\vec{D}$ is continuous across the interface [23]:

$$\vec{D}_{1,n} = \vec{D}_{2,n} \,. \tag{4}$$

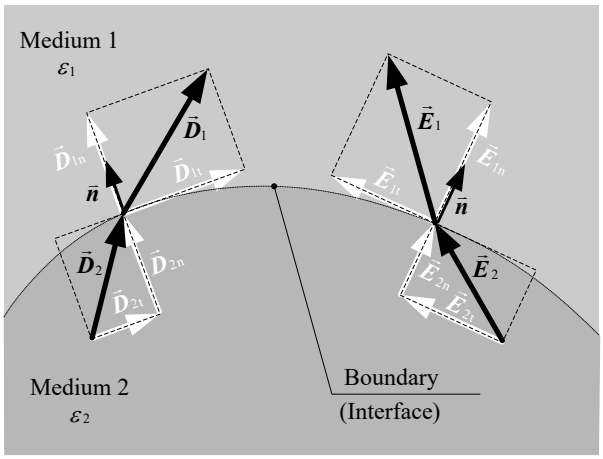

Figure 2 Graphical representation of boundary conditions for the electric field and electric displacement field at the interface of two media with different permitivities

4 MODELLING THE ELECTRIC FIELD OF THE GLASS INSULATOR

The space of interest for modelling is the space between the metal cap and the metal pin (Fig. 3 and 4). The inner cylinder represents the metal pin and the outer cylinder represents the metal cap. The space between these two metal cylinders is filled with a complex (heterogeneous) insulating material. That is, with the cement around the inner electrode, then with the glass, and again with the cement between the glass and the outer electrode. Each layer of the insulating material is represented by a hollow cylinder, and the cylinders are coaxial (Fig. 3 and 4).

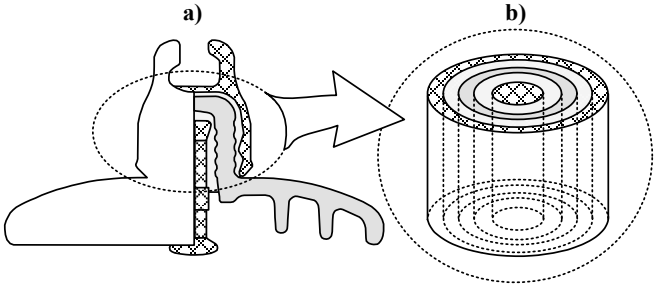

Figure 3 A sketch of the disc insulator and an equivalent system of coaxial electrodes with a complex dielectric between them

In the following text, are presented the key steps in deriving expressions for the E-field of a coaxial structure consisting of three dielectrics. The presented derivation is an extension of the typical derivation for E-fields of coaxial structures to the case of multiple dielectrics [22, 23]. The expressions presented for determining the electric field in the space between coaxial metal cylinders are derived assuming very long cylinders. However, when this is not the case, as in this article, the expressions provide an approximation of the electric field. Another limitation of the analytical approach is cement modelling. Electrical conductivity of cement (semi-conductive, Tab. 1) is high compared to insulating materials, which affects the field distribution.

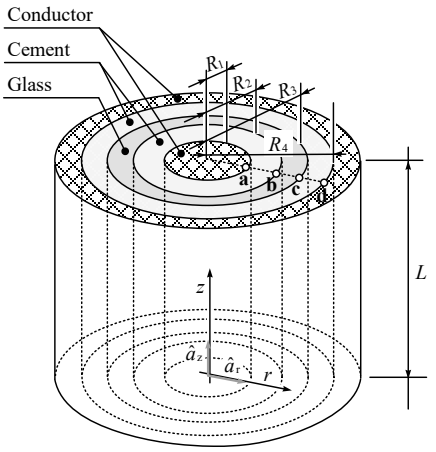

Figure 4 Detailed view of the equivalent system of coaxial electrodes with a complex dielectric between them

Since cylinders are initially assumed to be infinite in length, the electric field has only a radial component. The electric field is a function of the distance from the longitudinal axis of the coaxial cylinders and it also depends on the dielectric constant of the medium.

$$\vec{E}(r) = \begin{cases} E_1(r)\cdot\hat{a}_r \text{ for } R_1 \le r \le R_2, \\ E_2(r)\cdot\hat{a}_r \text{ for } R_2 \le r \le R_3, \\ E_3(r)\cdot\hat{a}_r \text{ for } R_3 \le r \le R_4, \end{cases} \tag{5}$$

where $\hat{a}_r$ is unit vector along the r axis. The electric field in the space around the inner electrode, a space filled with cement, is denoted by E_1. The electric field in the space filled with glass is denoted by E_2. The electric field in the space filled with cement (the space between the glass and the outer electrode) is denoted by E_3. The E-field in the space around a flat and very long cylindrical conductor is determined by the expression [22, 23]:

$$E_1(r) = \frac{\lambda}{2\pi\varepsilon_1}\cdot\frac{1}{r}, \tag{6}$$

where ε_1 is the permittivity of the medium in which the inner electrode is located (cement), r is radial distance from the longitudinal axis of the inner electrode and λ is line charge density. According to the boundary condition described by Eq. (4), the following applies:

$$D_1(R_2) = D_2(R_2), \tag{7}$$

$$D_2(R_3) = D_3(R_3). \tag{8}$$

Applying constitutive equation to expression (7) and (8), and taking into account (6), gives:

$$\vec{E}(r)=\begin{cases}\dfrac{\lambda}{2\pi\varepsilon_1}\cdot\dfrac{1}{r}\cdot\hat{a}_{\mathrm{r}} \text{ for } R_1\le r\le R_2,\\ \dfrac{\lambda}{2\pi\varepsilon_2}\cdot\dfrac{1}{r}\cdot\hat{a}_{\mathrm{r}} \text{ for } R_2\le r\le R_3,,\\ \dfrac{\lambda}{2\pi\varepsilon_1}\cdot\dfrac{1}{r}\cdot\hat{a}_{\mathrm{r}} \text{ for } R_3\le r\le R_4.\end{cases} \quad (9)$$

For the practical application of the previous expression, it is necessary to determine the line charge density λ. One way this can be done is presented below. The relationship between electric potential and electric field is described by the expression [22, 23]:

$$\vec{E}=-\mathrm{grad}\,\varphi. \quad (10)$$

By integrating the previous expression along the integration curve lying on the radial axis, the expression for the voltage between the outer and inner metal cylinders is obtained:

$$U_{da}=\varphi_d-\varphi_a=-\int_a^d\vec{E}\mathrm{d}\vec{s}\,. \quad (11)$$

Taking into account Eq. (9), the previous line integral with integration limits from *a* to *d*, needs to be broken down into three line integrals:

$$U_{da}=-\int_a^b\vec{E}_1\mathrm{d}\vec{s}-\int_b^c\vec{E}_2\mathrm{d}\vec{s}-\int_c^d\vec{E}_3\mathrm{d}\vec{s}\,. \quad (12)$$

Inserting Eq. (9) into the previous expression and after performing the integration gives:

$$U_{ad}=\frac{\lambda}{2\pi\varepsilon_1}\ln\frac{R_2}{R_1}+\frac{\lambda}{2\pi\varepsilon_2}\ln\frac{R_3}{R_2}+\frac{\lambda}{2\pi\varepsilon_1}\ln\frac{R_4}{R_3}. \quad (13)$$

The charge on the electrodes is determined by the expressions:

$$Q=C\cdot U_{ad}, \quad (14)$$

$$Q=\lambda\cdot L, \quad (15)$$

where λ is line charge density, C is capacitance, U_{ad} is voltage between the electrodes and L is cylinder length. Combining the previous two expressions gives:

$$\lambda=\frac{C\cdot U_{ad}}{L}, \quad (16)$$

$$C=\frac{2\pi L}{\frac{1}{\varepsilon_1}\ln\frac{R_2}{R_1}+\frac{1}{\varepsilon_2}\ln\frac{R_3}{R_2}+\frac{1}{\varepsilon_1}\ln\frac{R_4}{R_3}}. \quad (17)$$

Inserting of Eq. (17) into Eq. (16) gives:

$$\lambda=\frac{2\pi U_{ad}}{\frac{1}{\varepsilon_1}\ln\frac{R_2}{R_1}+\frac{1}{\varepsilon_2}\ln\frac{R_3}{R_2}+\frac{1}{\varepsilon_1}\ln\frac{R_4}{R_3}}. \quad (18)$$

Eq. (18), together with Eq. (9), allows the determination of the electric field in the space between the inner and outer electrodes. Typically, at 10 kV/400 V distribution tower, on the 10 kV side, two glass insulators are used per phase (Fig. 1). Voltage distribution, along the insulator string (glass or porcelain), is not linear due to stray capacitances. Therefore, the voltage in a two-unit string is not equally shared by each unit. Nevertheless, given the comparison of the results obtained by the analytical and numerical approach, it is sufficient to choose a reasonable value of voltage as input given for both calculation types. Therefore, voltage of 5 kV was adopted for the field calculation in the insulator.

The properties of insulating materials relevant for the analysis are summarized in Tab. 1 [25-27]. The field calculation was performed for values U_{ad} = 5 kV, ε_{r1} = 15 (cement), ε_{r2} = 5 (glass), ε_{r3} = ε_{r1} = 15 (cement), ε_0 = 8.854×10^{-12} F/m. According to the previously derived expressions, the calculation of the electric field in the area of interest was performed using software package Mathcad 14 [28]. Software package Mathcad was used to automate the process of calculations and obtain graphical representations. Other programs, such as Matlab, can be used for this purpose [29].

The results of the calculation using analytical expressions are shown in Fig. 9 and Fig. 11.

Table 1 Properties of materials relevant for insulator modelling

Material	Relative permitivity ε_r (-)	Electric conductivity σ (S/m)
Air	1,0	10^{-13} - 10^{-18}
Glass	4 - 6,5	10^{-11} - 10^{-15}
Cement	2 - 30	10^{-3} - 10^{-4}
Steel (cast)	1,0	5×10^{6}

5 FINITE ELEMENT ANALYSIS

In the calculation of the electric field with the finite element method, the same material properties were used as in the calculation with analytical expressions. For this purpose, commercial software Ansys based on the FEM was used [30]. Within the Ansys software package, the Maxwell module and the electrostatic solver were selected. The segmentation of the computational domain was done by limiting the number of elements to 10,000 elements. Next, selected is an adaptive solver setup with a maximum number of pass equal to 20 and a percentage error of 0.1%. The 2D Ansys model of the disc insulator with two paths, along which the electric field is calculated in particular detail, is shown in Fig. 5. The results of the calculation with FEM are shown in Figs. 6-8 and Fig. 10.

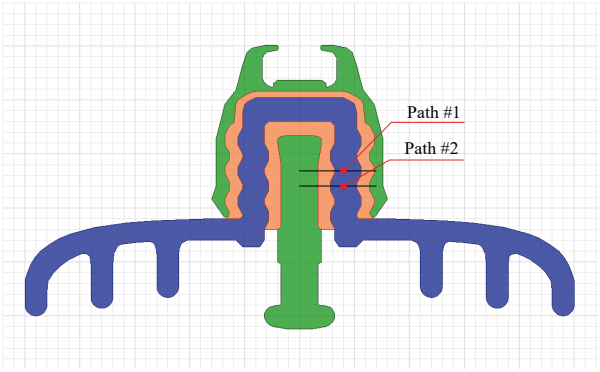

Figure 5 2D Ansys model of the disc insulator with two paths along which the electric field is calculated in particular detail

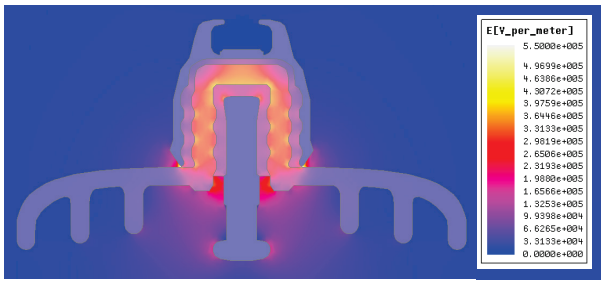

Figure 6 Distribution of the electric field inside and outside the disk insulator

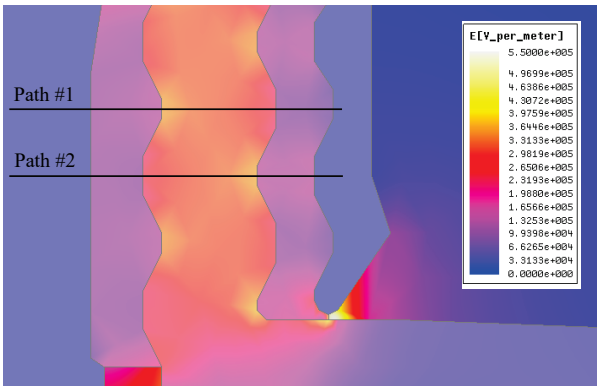

Figure 7 Distribution of the electric field inside and outside the disk insulator. Enlarged detail on the area between the metal pin and the metal cap

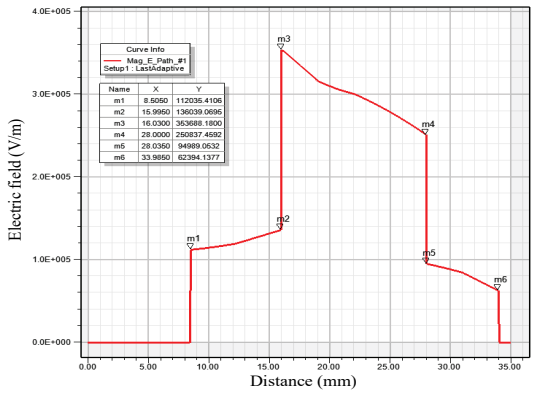

Figure 8 Electric field along path # 1 calculated by the finite element method

The electric field strengths at the boundary points between two media (insulating materials) determined by the finite element method and the analytical expressions are summarized in Tab. 2 and Tab. 3.

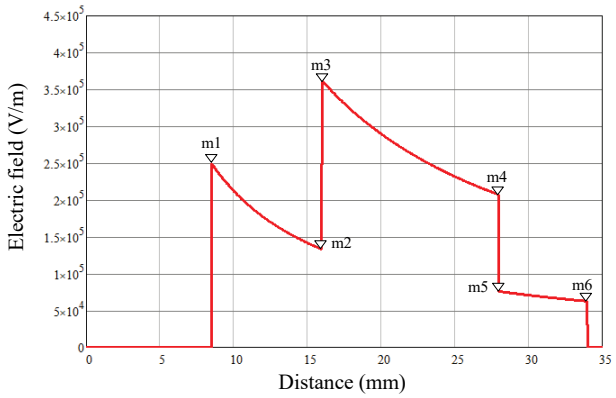

Figure 9 Electric field along path # 1 calculated by the analytical expressions

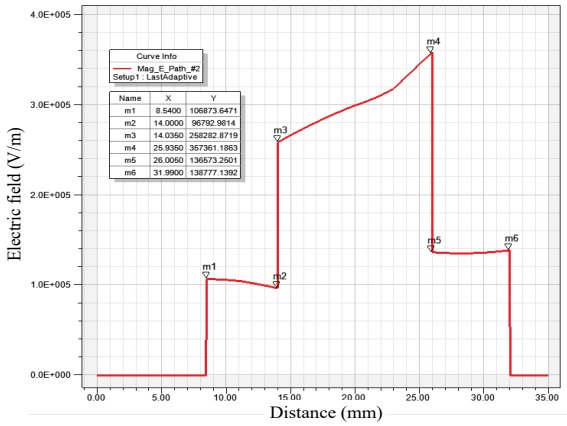

Figure 10 Electric field along path # 2 calculated by the finite element method

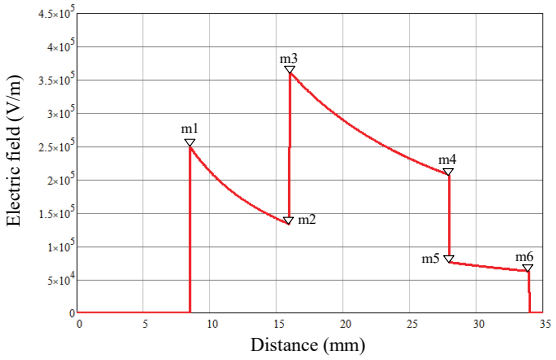

Figure 11 Electric field along path # 2 calculated by the analytical expressions

Table 2 Electric field along path # 1 at points of discontinuity *, **

Radial distance	Marker	Electric field (kV/m)	
		FEM	Analytic
R_{1+}	m1	112	250
R_{2-}	m2	136	134
R_{2+}	m3	354	362
R_{3-}	m4	251	208
R_{3+}	m5	95	76
R_{4-}	m6	62	63

* $R_1 = 8{,}5$ mm, $R_2 = 16$ mm, $R_3 = 28$ mm, $R_4 = 34$ mm

** $R_+ = \lim_{\Delta R \to 0}(R + \Delta R)$, $R_- = \lim_{\Delta R \to 0}(R - \Delta R)$

Table 3 Electric field along path # 2 at points of discontinuity *, **

Radial distance	Marker	Electric field (kV/m)	
		FEM	Analytic
R_{1+}	m1	107	246
R_{2-}	m2	97	150
R_{2+}	m3	258	407
R_{3-}	m4	357	220
R_{3+}	m5	137	80
R_{4-}	m6	139	65

* R_1 = 8,5 mm, R_2 = 14 mm, R_3 = 26 mm, R_4 = 32 mm

** $R_+ = \lim_{\Delta R \to 0}(R + \Delta R)$, $R_- = \lim_{\Delta R \to 0}(R - \Delta R)$

6 ANALYSIS OF RESULTS

When analyzing the results obtained by the analytical expressions and FEM, the results obtained by FEM are considered accurate and the results obtained by the analytical expressions are considered approximate. Theoretically, there are several physical phenomena that affect the distribution of the electric field in the space between the metal cap and the metal pin of the glass pane insulator. It is known from electrostatics that on the surface of conductive bodies the charge concentration is higher in areas with smaller radius of curvature such as edges, spikes, ends of elongated bodies, etc. In the case of disk insulators, the increased charge concentrations are found at both ends of the metal pin and at the opening of the metal cap (Fig. 6 and Fig. 7). For this reason, the analytical expressions presented are not valid (applicable) for calculating the electric field in the immediate vicinity of the end of the metal pin inside the metal cap, nor are they valid (applicable) for calculating the electric field in the immediate vicinity of the opening of the metal cap. In addition, there is another phenomenon that significantly affects the distribution of the electric field in the considered part of the space. In order to mechanically strengthen the connection of the metal cap with the rest of the insulator, the inner surface of the metal cap has a corrugated (fluted) cross-section. Therefore, the insulating materials (glass and cement) inside the cap have the same wavy pattern. Due to the change in the radius of curvature on the inside of the metal cap, the charge concentration is non-uniform along the inner surface of the metal cap. In convex areas, the charge concentration is higher than in concave areas. Therefore, the electric field strength along the inner surface of the metal cap is higher in convex regions than in concave regions.

According to the analytical expressions, the E-field may exhibit sudden (sharp) jumps at dielectric boundaries, but the E-field always decreases monotonically as the radial distance increases. Such a global trend of E-field behavior is disturbed by the local influence of non-uniform charge concentration on convex and concave zones of the inner surface of the metal cap. If the path, along which the E-field is analyzed, coincides with the concave zone of the inner surface of the metal cap, as in path #1, the waveforms of the E-field obtained by the finite element method and analytical expressions are similar (Fig. 8 and Fig. 9). When the path, along which the E-field is analyzed, coincides with the convex zone of the inner surface of the metal cap, as in path # 2, the waveforms of the E-field obtained by the finite element method and analytical expressions differ drastically (Fig. 10 and Fig. 11).

The numerical values of the E-field (Figs. 8 - 11, Tab. 2 and Tab. 3) show that the numerical values obtained with FEM and the analytical expressions are of the same order of magnitude. Although the analytical expressions provide approximate values, these values are physically meaningful. As such, they are useful for theoretical considerations and can be used in the initial stages of insulator design. However, for more detailed analysis and design, it is inevitable to use FEM.

7 RECAPITULATION ANNOTATION

Investigating the possibility of describing E-fields with simple analytical expressions, such as those used in coaxial capacitors to describe E-fields in HV glass disk insulators, can be done relatively easily at the analytical level. The space between the metal cap and the metal pin is represented as a complex dielectric. Analytical expressions for the electric field in these dielectrics are derived. The applicability of the presented expressions was verified by numerical calculations using the finite element method. In this work, the significant influence of convex and concave zones on the inner surface of the metal cap on the electric field distribution in the space between the metal pin and the metal cap was demonstrated. The work showed that it is possible to determine the approximate distribution of the electric field in the space between the metal pin and the metal cap of the glass insulator using the analytical expressions presented. However, the article also pointed to the limitations of the analytical expressions. Therefore, the presented analytical expressions have their theoretical meaning and can be useful in the initial stage of glass insulator design. The finite element method once again proved its superiority and proved to be an indispensable tool for the analysis and design of glass insulators.

Acknowledgments

This research is supported by the European Union from the European Regional Development Fund within the Operational Program "Competitiveness and Cohesion 2014-2020", under the project entitled Research and development of systems for monitoring high-voltage routes, and especially the discharge of high-voltage insulators using IoT technologies, under the project number KK.01.2.1.02.0056.

8 REFERENCES

[1] James, R. E. & Su, Q. (2008). *Condition Assessment of High Voltage Insulation in Power System Equipment*. The Institution of Engineering and Technology. https://doi.org/10.1049/PBPO053E

[2] Macey, R. E., Vosloo, W. L. & De Tourreil, C. (2004). *The practical guide to outdoor high voltage insulators.* Crown Publications.

[3] Kind, D. & Kärner, H. (1985). *High-Voltage Insulation Technology*. Springer Fachmedien Wiesbaden GmbH. https://doi.org/10.1007/978-3-663-14090-0

[4] Khan, M. J. (1980). *Computation of electric fields in and around high voltage insulators*. Master Thesis, Department of Electrical and Computer Engineering, University of Windsor.
[5] Rienen van U. (2001). *Numerical Methods in Computational Electrodynamics.* Springer, 1st edition. https://doi.org/10.1007/978-3-642-56802-2
[6] Schilders, W. H. A. & Maten, E. J. W. (2005). *Numerical Methods in Electromagnetics*. North Holland, 1st edition.
[7] Sadiku, M. N. O. (2000). *Numerical Techniques in Electromagnetics*. CRC Press, 2nd edition. https://doi.org/10.1201/9781420058277
[8] Mujezinović, A., Čarsimamović, A., Čarsimamović, S., Muharemović, A. & Turković, I. (2014). Electric field calculation around of overhead transmission lines in Bosnia and Herzegovina. *2014 International Symposium on Electromagnetic Compatibility*, Gothenburg, Sweden, 1001-1006. https://doi.org/10.1109/EMCEurope.2014.6931049
[9] Virbalis, J. A., Marciulionis, P., Lukocius, R., Deltuva, R. & Nedzinskaite, G. (2015). Analytical Expression of Electric Field Strength under Three–Phase Line. *International Journal of Advanced Research in Electrical, Electronics and Instrumentation Engineering*, *4*(8), 7176-7182. https://doi.org/10.15662/ijareeie.2015.0408087
[10] Micu, D. D., Ceclan, A., Darabant, L. & Stet, D. (2009). Analytical and Numerical Development of the Electromagnetic Interference between a High-Voltage Power Line and a Metallic Underground Pipeline. *2009 8th International Symposium on Advanced Electromechanical Motion Systems & Electric Drives Joint Symposium*, Lillie, France, 1-6, https://doi.org/10.1109/ELECTROMOTION.2009.5259090
[11] El-Hawary, M. E. (2008). *Introduction to Electrical Power Systems.* Wiley-IEEE Press. https://doi.org/10.1002/9780470411377
[12] Malik, N. H., Al-Arainy, A. A., Qureshi, M. I. & Pazheri, F. R. (2011). Calculation of Electric Field Distribution at High Voltage Cable Terminations. *Journal of Energy Technologies and Policy*, *1*(2), 1-10. ISSN 2225-0573
[13] Christoph, J. & Clemens, M. (2019). Electric Field Model at Interfaces in High Voltage Cable Systems. *19th International Symposium on Electromagnetic Fields in Mechatronics, Electrical and Electronic Engineering (ISEF)*. https://doi.org/10.1109/ISEF45929.2019.9097007
[14] Soares, D. M., Mendonça, S., Neto, E. T. W. & Martinez, M. L. B. (2016). Electrical field on non-ceramic insulators and its relation to contact angles for constant volume droplets. *Journal of Electrostatics*, *84*, 97-105. https://doi.org/10.1016/j.elstat.2016.10.001
[15] Saleem, M. Z. & Akbar M. (2022). Review of the Performance of High-Voltage Composite Insulators. *Polymers, 14*(3), 431. https://doi.org/10.3390/polym14030431
[16] Pleşa, I., Noţingher, P., Schlögl, S., Sumereder, C. & Muhr, M. (2016). Properties of Polymer Composites Used in High-Voltage Applications. *Polymers, 8*(5), 173. https://doi.org/10.3390/polym8050173
[17] Sundararajan, R. & Gorur, R. S. (1994). Effect of insulator profiles on DC flashover voltage under polluted conditions. A study using a dynamic arc model. *IEEE Transactions on Dielectrics and Electrical Insulation, 1*(1), 124-132. https://doi.org/10.1109/94.300239
[18] Ramos, G. N., Campillo, M. T. R. & Naito, K. (1993). A study on the characteristics of various conductive contaminants accumulated on high voltage insulators. *IEEE Transactions on Power Delivery*, *8*(4) 1842-1850. https://doi.org/10.1109/61.248293
[19] Mizuno, Y., Kusada, H. & Naito, K. (1997). Effect of climatic conditions on contamination flashover voltage of insulators. *IEEE Transactions on Dielectrics and Electrical Insulation, 4*(3), 286-289. https://doi.org/10.1109/94.598284
[20] Sediver. (2021). Toughened glass insulators for HVAC applications. https://www.sediver.com
[21] JSC U.M.E.K. (2023). Toughened glass suspension insulator. https://umek.pro/products/catalogues
[22] Hayt, W. H. & Buck, J. A. (2001). *Engineering Electromagnetics*. McGraw-Hill Science/Engineering/Math, 6th edition.
[23] Haznadar, Z. & Štih, Ž. (2000). *Electromagnetic Fields, Waves, and Numerical Methods*. IOS Press.
[24] Sadiku, M. N. O. (2018). *Elements of Electromagnetics*. Oxford University Press, 7th edition.
[25] Uckol, H. I., Karaca, B. & Ilhan, S. (2020). DC and AC electric field analysis and experimental verification of a silicone rubber insulator. *Electrical Engineering, 102*, 503-514. https://doi.org/10.1007/s00202-020-00954-3
[26] Matmatch. (2023). Matmatch is a materials search platform. https://matmatch.com
[27] Totalmateria. (2023). Totalmateria is comprehensive materials Database. https://www.totalmateria.com
[28] Mathcad. (2023). Math Software for Engineering Calculations. https://www.mathcad.com/en
[29] MathWorks, Matlab. (2023). Matlab is a programming and numeric computing platform. https://www.mathworks.com/products/matlab.html
[30] Ansys. (2023). Engineering simulation and 3D design software. https://www.ansys.com

Authors' contacts:

Tomislav Barić, Full professor, PhD
Faculty of Electrical Engineering, Computer Science and Information Technology Osijek, University of Osijek,
Kneza Trpimira 2B, 31000 Osijek, Croatia
E-mail: tomislav.baric@ferit.hr

Hrvoje Glavaš, Full professor, PhD
Faculty of Electrical Engineering, Computer Science and Information Technology Osijek, University of Osijek,
Kneza Trpimira 2B, 31000 Osijek, Croatia
E-mail: hrvoje.glavas@ferit.hr

Željko Hederić, Full professor, PhD
Faculty of Electrical Engineering, Computer Science and Information Technology Osijek, University of Osijek,
Kneza Trpimira 2B, 31000 Osijek, Croatia
E-mail: zeljko.hederic@ferit.hr

Mirko Karakašić, Full professor, PhD
(Corresponding author)
University of Slavonski Brod, Mechanical Engineering Faculty in Slavonski Brod,
Trg Ivane Brlić-Mažuranić 2, 35000 Slavonski Brod, Croatia
E-mail: mirko.karakasic@unisb.hr